International Journal on Advanced Science Engineering Information Technology

Vol.9 (2019) No. 6
ISSN: 2088-5334

An Unscented Kalman Filter-based Synchronization Control Approach for Communication-Based Train Control Systems

Ismail Faruqi[#], M. Brahma Waluya[#], Yul Yunazwin Nazaruddin[#,£],Tua Agustinus Tamba[*,£], Augie Widyotriatmo[#]

[#]*Instrumentation and Control Research Group, Institut Teknologi Bandung, Bandung 40142, Indonesia*
E-mail: yul@tf.itb.ac.id

**Department of Electrical Engineering, Parahyangan Catholic University, Bandung 40141, Indonesia*
Corresponding E-mail: ttamba@unpar.ac.id

[£]*National Center for Sustainable Transportation Technology (NCSTT), Bandung 40132, Indonesia*

***Abstract*—Communication-based train control (CBTC) system is an advanced train signalling and control technology which is developed using the *moving block signalling* (MBS) framework. The CBTC system has been shown to be capable of improving the operational efficiency, line capacity and safety of the railway operation. The main objective in implementing the MBS framework in CBTC system is to minimize the train headways through the utilization of an inter-train continuous communication system that determine and control the position of each train more precisely. One important challenge in such an implementation is the fulfillment of the necessary requirement of having highly accurate train localization method to ensure the safety of the short headway operation. This paper describes the results from experimental examination and application of a synchronization control strategy for the CBTC system using an unscented Kalman filter (UKF)-based sensor fusion approach as the localization method. In the proposed approach, the train localization task is performed using an UKF-based sensor fusion method which fuses measurement data from speed sensors and radio frequency identification tags. A synchronization control approach to ensure the safety movement of the train convoy in curved railway tracks under the MBS scheme is then proposed. The results presented in this paper show that the proposed localization and synchronization control methods can significantly improve the localization accuracy and reduce the inter-train headways.**

***Keywords*— CBTC; moving block signaling; synchronization control; unscented Kalman filter.**

I. INTRODUCTION

The demand for more efficient rail transportation systems is currently increasing in Indonesia, especially in densely populated regions such as the Greater Jakarta area of the DKI Jakarta province. For instance, the currently operating KRL Commuterline (KRLC) that serves Jakarta and its neighboring cities has for a while, been facing the issue of overcapacity. A recent report [1] has shown that the operational load of the KRLC in 2017 has reached as much as 860,000 passengers/day (with a 17% annual growth rate) and caused significant overcapacity during the peak operational hours. Such an overcapacity is further complicated by the suboptimal operational efficiency of the train traffic due to the use of aged signaling and control systems with degraded performance. Increasing the line capacity and at the same time ensuring the operational safety of the railway transportation systems such as KRLC are therefore among the most essential issues in Indonesian rail transport systems development.

The CBTC system is a modern advanced train signaling and control technologies which have been developed under the framework of MBS scheme [2]–[4]. Unlike the more traditional *Fixed Block Signaling* (FBS) scheme which partitions the rail track into several fixed/static sections or segments named "blocks" to determine the occupancy status of each of such blocks (cf. Fig. 1), the MBS scheme uses a continuous communication system which connects each train on the track and the wayside signaling equipment to dynamically separate and maintain a safe distance between adjacent trains based on a predefined safe operational scenario [2] (cf. Fig. 2). The MBS scheme has been shown to be capable of significantly reducing the headway of adjacent trains and thus increasing the track line capacity. To ensure the accuracy and safety of the MBS scheme implementation in CBTC system, reliable train localization and control modules are inevitably needed.

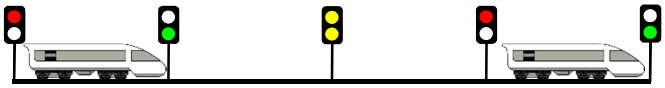

Fig. 1 Fixed Block Signaling (FBS) scheme.

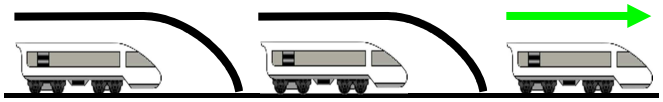

Fig. 2 Moving Block Signaling (MBS) scheme.

The standard approach to perform the train localization task in the conventional FBS scheme mainly relies on the use of a track detection sensor such as track circuit or axle counter [3], [4]. The main limitation of this approach is that it is a static method which can only determine the occupancy status of a track segment (i.e. it does not provide real-time information about the exact position of each train in the occupied track segment). In order to implement the MBS scheme which requires real-time and accurate train position information, more reliable train localization methods are strictly needed. One such method is the *sensor fusion* (SF) [5] approach which combines data from various sensors to produce more accurate real-time localization information of moving objects such as trains. The SF method has been widely applied for real-time localization purposes in the fields of robotics and unmanned autonomous systems. Many research results have particularly reported that the SF-based localization results are generally more accurate and reliable than those obtained using only individual sensor information. In railway system applications, the SF-based localization method was first introduced in [6] using linear Kalman filter (KF) framework. Various SF-based localization methods were subsequently developed using such methods as extended Kalman filter (EKF) [7] and its combination with GNSS [8]–[10], map matching [11], probabilistic weighted fusion [12], visual-aided odometry [13], particle filtering [14] and probabilistic data fusion [15]. See e.g. [16] for a recent survey on train localization methods and developments.

This paper reports the results of an experimental study and application of a SF-based synchronization control approach for the MBS-based CBTC system. In the proposed approach, the train localization task is performed using an UKF-based SF method. As shown in [17]–[22], the UKF often gives better estimation results than those obtained by the EKF method, especially in the case highly nonlinear systems. In this paper, the UKF method is used to fuse measurement data from speed sensors and radio frequency identification (RFID) tags. As for the control algorithm, this paper develops an extension of a previously developed synchronization control approach [23] to allow its use on more general curved track lines. Experimental results which demonstrate the performance of the proposed methods on a CBTC prototype are reported.

II. Materials and Methods

This section presents the materials and methods that were used for implementing an UKF SF-based synchronization control method on a lab scale CBTC miniature prototype.

A. Materials

Two train miniatures, denoted as train A and B are used in the experiment to perform the MBS scheme operation. As shown in Fig. 3, three stations are defined on the track, namely the main station, station A and station B. The main station is where both trains can stop while each of the remaining two is where the corresponding train can stop. In the experiment, each train will stop twice (each for a few seconds), the first at the main station and the second at their respective station.

Each of the two train miniatures is equipped with encoder while twelve RFID readers and a NodeMCU microcontroller are used as wayside sensor and onboard controller. The RFID tags play the role of balises in real railway system, whereas the NodeMCU collects all sensor data and then send them to a computer located in the wayside unit through a wireless communication link and MQTT protocol. Inside the computer, the UKF-based SF algorithm is coded in Matlab. The localization algorithm is first developed to predict the train position using train speed data from encoder. Once the RFID data are available, the predicted position will then be calibrated using the proposed UKF-based SF method. Fig. 4 depicts the architecture of the experimental setup.

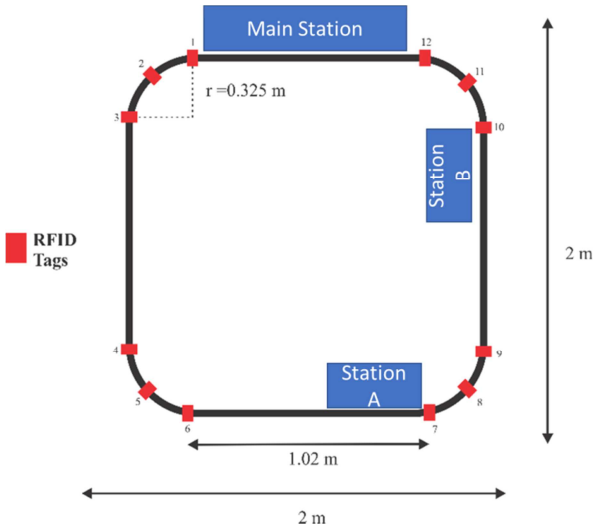

Fig. 3 Track dimension and RFID tags placement.

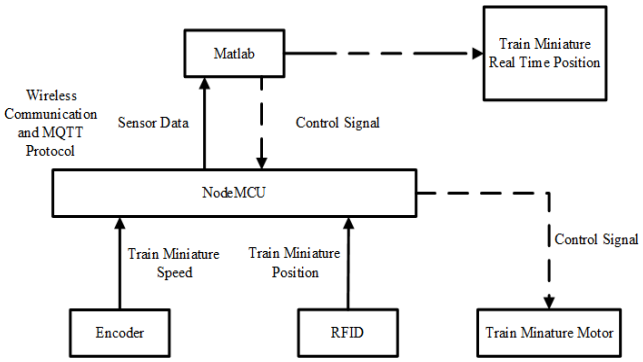

Fig. 4 System architecture for SF implementation.

B. Methods

In this section, the basic algorithm of discrete-time UKF that is used for implementing the SF method is presented. Discrete-Time UKG Algorithm: In essence, the UKF is a

Bayesian-type estimation method which uses a probabilistic transformation to approximate the statistics of nonlinear systems [17]–[19]. Unlike the EKF method which propagates the states distribution through the first order linearization of the system dynamics, the UKF method instead generates a minimal set of carefully chosen sample points of the states distribution and then transforms them directly through the system model. Such sample points, also known as sigma points, are chosen to capture the true first two moments of the state distribution. As such, when propagated through the system model (cf. Fig. 5), these points will also capture the posterior distribution of the system's moments. In this regard, the UKF method does not suffer the linearization-induced suboptimality issue that often occurs in EKF implementation.

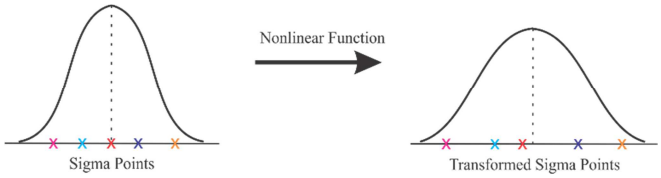

Fig. 5 An illustration of the sigma points transformation.

The algorithmic implementation of the UKF is initialized with a set guesses on initial mean and covariance of the state variables, and afterward followed by two main steps, namely prediction and correction steps. The prediction step aims to estimate the future values of the state variables and output based on the results of sigma points transformation. When actual measurements are available, the algorithm switches to the correction step which updates the previously obtained state and output predictions. These steps are then executed recursively whenever new measurement data are available.

To describe the algorithmic implementation of the UKF, consider the following discrete-time nonlinear system model.

$$x(k) = f(x(k-1), u(k-1), w) \tag{1}$$

$$y(k) = h(x(k-1), q) \tag{2}$$

where $x(k), u(k)$ and $y(k)$ denote the state, input, and output variables, respectively, at discrete time step *k*, while *w* and *q* are the process and measurement noises, respectively. Let $\hat{x}_0$ and P_0, respectively, denote the initial mean and covariance of the state variables. Then the initial probability density function of the state variables can be defined and the recursion steps in the UKF can be performed in the following steps (cf. [22], [23]).

1) Prediction Step: The prediction step essentially performs the recursion of three tasks, namely state variables prediction, output variable prediction and Kalman gain calculation. Select the initial set of sigma points $\mathcal{X}_0$ and its weight W_i to capture the PDF of the state variables. These may for instance take the following forms.

$$\chi_0 = \hat{x}(k-1 \mid k-1), \tag{3}$$

$$W_0 = j/(N_x + j), \tag{4}$$

In addition, the values of (3)-(4) at the *k*-th time step for the *i*-th state variables may be determined as follows.

$$\chi_i = \hat{x}(k-1 \mid k-1) + \sqrt{(N_x + j)P(k-1 \mid k-1)}, \tag{5}$$

$$W_i = j/2(N_x + j), \tag{6}$$

where N_x denotes the dimension of state variables and $j = 3 - N_x$ is a scaling parameter. These sigma points and weights may then be transformed using the system model in (1) to obtain a predicted value of the form

$$\chi_i(k \mid k-1) = f(\chi_i(k-1 \mid k-1), u(k-1), w), \tag{7}$$

In this regard, the mean of the state variables can be determined using the so-called *weighted statistical linear regression* (WSLR) method to obtain

$$\hat{x}(k \mid k-1) = \sum_{i=1}^{2N_x} W_i \chi_i(k \mid k-1). \tag{8}$$

As a result, the prediction error $(e_{\hat{x}_i})$ and covariance $(P(k|k-1))$ may then be determined as

$$e_{\hat{x}_i} = \chi_i(k \mid k-1) - \hat{x}(k \mid k-1), \tag{9}$$

$$P(k \mid k-1) = \sum_{i=1}^{2N_x} W_i [e_{\hat{x}_i}][e_{\hat{x}_i}]' + R_W, \tag{10}$$

where R_w denotes the process noise covariance matrix.

Using the state variables prediction, a set of sigma points $\mathcal{Y}$ for the output variables can be determined as

$$\mathrm{Y}_0(k-1 \mid k-1) = \chi_i(k \mid k-1), \tag{11}$$

$$\mathrm{Y}_i(k-1 \mid k-1) = \chi_i(k \mid k-1) + j\sqrt{R_w(k \mid k-1)}, \tag{12}$$

with similar weighting values as the state variables sigma points. Correspondingly, the predicted sigma points of the output variables may be obtained by transforming them through the system's output model in (2) to obtain

$$\mathrm{Y}_i(k \mid k-1) = h(\mathrm{Y}_i(k-1 \mid k-1), q). \tag{13}$$

Using the WSLR method, the predicted output variables may then be computed as

$$\hat{y}(k \mid k-1) = \sum_{i=1}^{2N_X} W_i \mathrm{Y}_i(k \mid k-1). \tag{14}$$

The residual error $\epsilon_i(k|k-1)$ and residual covariance $R_\epsilon(k|k-1)$ of the output prediction are thus given by

$$\varepsilon_i(k \mid k-1) = \mathrm{Y}_i(k \mid k-1) - \hat{y}(k \mid k-1), \tag{15}$$

$$R_\varepsilon(k \mid k-1) = \sum_{i=1}^{2N_x} W_i [\varepsilon_i(k \mid k-1)][\varepsilon_i(k \mid k-1)]' + R_q. \tag{16}$$

where R_q is the measurement noise covariance matrix.

Based on the obtained prediction of the state and output variables, the prediction of the cross covariance may then be determined as follows.

$$R_{x\varepsilon}(k \mid k-1) = \sum_{i=1}^{2N_x} W_i [e_{\hat{x}_i}(k \mid k-1)][e_{\hat{x}_i}(k \mid k-1)]' + R_q \quad (17)$$

At this point, the Kalman gain of the UKF may then be determined and updated recursively as

$$K(k) = R_{x\varepsilon}(k \mid k-1) R_{x\varepsilon}^{-1}(k \mid k-1). \quad (18)$$

2) Correction Step: The correction step utilizes the actual measurement data from sensors ($z(k)$) to make corrections on the computed state variables and output predictions. By using a similar routine as in the generic KF method, the correction begins with the calculation of the innovation variable of the form

$$\Theta(k) = z(k) - \hat{y}(k \mid k-1). \quad (19)$$

Using the innovation $o(k)$, the correction on the predicted state variables and covariance can be performed as follows.

$$\hat{x}(k \mid k) = \hat{x}(k \mid k-1) + K(k)\Theta(k), \quad (20)$$

$$P(k \mid k) = P(k \mid k-1) - K(k) R_{\varepsilon}(k \mid k-1) K'(k). \quad (21)$$

The corrected values of the state variables and covariance prediction are then used in the next recursion of prediction-correction iteration [17]–[22].

- Synchronization Control of CBTC Systems:

The CBTC system generally consists of three major components, namely the wayside unit, on-board unit, and radio communication module between wayside and on-board units [2]–[4], [24]. The on-board unit consists of (i) on-board position sensors and (ii) computers which process all such sensors and use them to control the train speed. The wayside unit contains (i) the so-called automatic train supervision (ATS) system which controls all the operated trains, (ii) a zone controller and interlocking system which manage some predetermined areas in certain track line, and (iii) positioning tags which calibrate the train position as determined by the on-board unit.

The MBS-based CBTC implementation relies on the so-called *movement authority* which essentially is a real-time information exchange system that provides to each train real-time location data as well as command of movement among trains along a track segment/area [24]. While the MBS-based CBTC has the potential to increase the line capacity, its current implementation does not provide a synchronization scheme which can ensure the attainment of a minimum possible headway among adjacent trains. The synchronization control scheme has been proposed for MBS-based CBTC but its implementation remains limited to straight line track topology [23]. In this work, we extend the approach to allow its implementation on more general curved track lines through the development of an algorithm which maps curved train segments into appropriate and equivalent straight-line track segment.

The main objective of synchronization control approach in MBS-based CBTC system is to dynamically separate adjacent trains by a minimum safety distance and then maintain such a condition for a certain duration of time. The theoretical development of this approach was developed in [23] for a particular form of straight-line track. The basic idea in that approach is illustrated in Fig. 6 which shows that the controller will be activated whenever a train enters a safe distance zone as measured relative to the train in front of it. In particular, the controller will automatically adjust the braking of the following train, slowing it down or accelerating it up until a stable minimum distance is achieved [23], [24].

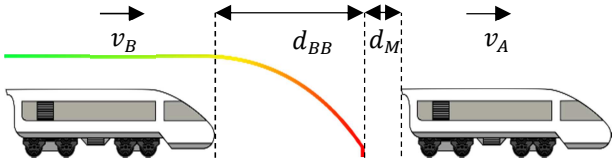

Fig. 6 Activation of the synchronization control.

Regarding the Figure 6, we define the notion of *safety margin* (d_M) as the measured distance between the tail (x_{AT}) and the nose (x_{BN}) of adjacent trains when they are at rest. Furthermore, we also define the *braking distance* d_{BB} as an estimated travelled distance after a train hits the brakes until a complete stop, i.e.:

$$d_{BB}(x_B(k), v_B(k)) = v_B^2 / 2\beta_s. \quad (22)$$

where $x_B(k)$ and $v_B(k)$ denote, respectively, the position and velocity of the train *B*, and β_s is the maximum braking rate of the train (cf. Fig. 6). Now, we define the so-called *minimum distance* ($d_{\min}(k)$) of the synchronization as the sum of the safety margin (d_M) and the braking distance (d_{BB}), i.e.:

$$d_{\min}(k) = x_{AT} - x_{BN} = d_M + d_{BB}(x_B(k), v_B(k)). \quad (23)$$

In the MBS scheme implementation, the leading train can halt suddenly and is thus has a resemblance to the *brick walls* phenomenon [4]. Under this assumption, the braking or decelerating dynamics of the following train (β_B) can be derived by differentiating (25) to obtain

$$\frac{dx_{AT}}{dk} - \frac{dx_{BN}}{dk} = \frac{d}{dk} d_{BB}(x_B(k), v_B(k)), \quad (24)$$

$$v_a(k) - v_B(k) = \frac{\partial d_{BB}}{\partial x_B} v_B(k) - \frac{\partial d_{BB}}{\partial v_B} \beta_B(k) \quad (25)$$

$$\beta_B(k) = \left[\left(\frac{\partial d_{BB}}{\partial x_B} + 1 \right) v_B(k) - v_A(k) \right] \Big/ \left(\frac{\partial d_{BB}}{\partial v_B} \right), \quad (26)$$

where β_B is the the deceleration of the following train. As a result, the value of β_B can be determined from (26) as

$$\beta_B(k) = \beta_S \frac{v_B(k) - v_A(k)}{v_B(k)}, \quad (27)$$

with $v_B \neq 0$ is assumed to hold. In the case where adjacent trains start to move from rest (both train speed is zero), the

acceleration of the leading (α_A) and the following train (α_B) can be computed as

$$\alpha_A(k) = k_{acc}\beta_S, \tag{28}$$

$$\alpha_B(k) = \beta_S \frac{-1+\sqrt{1+4k_{acc}}}{2} \tag{29}$$

where k_{acc} is a constant.

- Experimental Consideration:

Several considerations are considered when implementing the proposed UKF SF-based synchronization control method on a lab scale CBTC system miniature track prototype as shown in Fig. 3. First, following the setup of the UKF method as described in Section II.B.1, a model for the train miniature is derived. In this regard, the train miniature is modeled as a rigid body with the following planar kinematic equation.

$$\begin{bmatrix} p_k^x \\ p_k^y \end{bmatrix} = \begin{bmatrix} 1 & 0 \\ 0 & 1 \end{bmatrix} \begin{bmatrix} p_{k-1}^x \\ p_{k-1}^y \end{bmatrix} + \begin{bmatrix} dt_{k-1}\cos(\theta_{k-1}) \\ dt_{k-1}\sin(\theta_{k-1}) \end{bmatrix} v_{k-1} \tag{30}$$

where p_k^x and p_k^y denote, respectively, the Cartesian basis and ordinate positions of the train at time k on the track, θ_k is the train orientation, and v_k denotes the train speed. The train kinematic contains nonlinearities in the form of trigonometric functions.

A fusion scheme as shown in Fig. 7 was then developed to process the collected sensor data. This diagram shows that two sensors are used in the experiment, i.e. encoder to measure the train speed and RFID tag readers to detect the train exact position. From the characteristics of these sensors, we found that the exact form of the train kinematic model in (30) is given by the following formula.

$$\begin{bmatrix} p_k^x \\ p_k^y \end{bmatrix} = \begin{bmatrix} 1 & 0 \\ 0 & 1 \end{bmatrix} \begin{bmatrix} p_{k-1}^x \\ p_{k-1}^y \end{bmatrix} + 0{,}3 \begin{bmatrix} \cos(\theta_{k-1}) \\ \sin(\theta_{k-1}) \end{bmatrix} \tag{31}$$

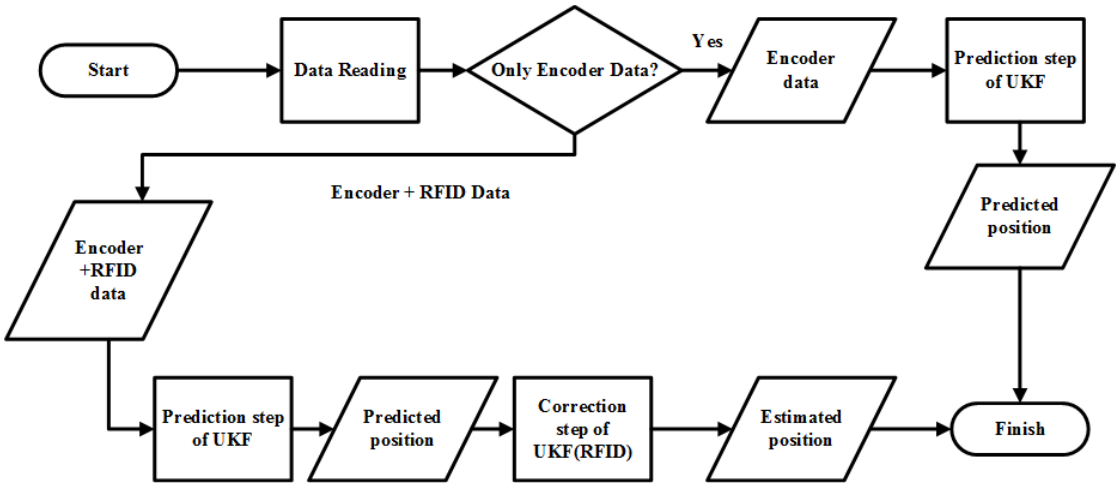

Fig. 7 Sensor fusion scheme applied in the experiment.

Using the obtained system model, the UKF procedure for SF task can be implemented. The set of sigma points, weight, and residual covariance for the implementation are defined below. The values of related parameters in these equations are summarized in Table 1. With these experimental model and parameters, the UKF-based SF procedure described in Section II.B.1 can be executed.

$$\chi_i' = \chi_0 + \alpha_{ukf}(\chi_i - \chi_0) \tag{32}$$

$$W_i' = \begin{cases} \frac{W_0}{\alpha_{ukf}^2} + \left(\frac{1}{\alpha_{ukf}^2} - 1\right), & i = 0 \\ \frac{Wi}{\alpha_{ukf}^2}, & i \neq 0 \end{cases} \tag{33}$$

$$R_\varepsilon' = \left(W_0 + 1 + \beta_{ukf} - \alpha_{ukf}^2\right)(\mathrm{Y}_0 - \hat{y})'(\mathrm{Y}_0 - \hat{y}) + R_\varepsilon \tag{34}$$

TABLE I
UKF PARAMETER USED IN THE ALGORITHM

UKF Parameter		
Parameter	Value	Notes
σ_enc:σ_RFID	7:400	Standard deviation of the used sensors. Smaller value indicates better accuracy and reliability.
α_ukf	0.001	Represent the sigma points distribution with respect to the mean value. Small value means close-to-mean sigma points.
β_ukf	2	Represents the system distribution where a value of 2 means Gaussian distribution

Secondly, the implementation of the synchronization control for MBS-based scheme was performed based on the following scenario and rules.

- The two trains depart from the same initial station
- The following train maintains the safe distance with the leading train and must stop when the leading train is picking up passengers at a station

- Both train arrive at the same station

Essentially, these conditions are used to ensure a *Collison*-free operation of the trains. The used synchronization control algorithm receives the train position (x_A and x_B) from the UKF-based SF result, whereas the train speed (v_A and v_B) are determined from encoder sensor data. The synchronization control task is evaluated using a predefined safe distance parameter of $d_{\min}(k) = 27cm$ and an acceleration rate of $k_{acc} = -1$. The chosen minimum distance essentially sets the inter-train minimum distance to be the same as the train length. Based on the described synchronization control approach, the acceleration/deacceleration rate (β_B) of the following train can be determined and then sent to the actuating motor to be calibrated to a train speed value (v_B) of the form

$$v_B(k+1) = v_B(k) + \beta_B(k)\Delta t, \tag{35}$$

where Δt is the sampling time of the encoder.

III. Results and Discussion

A. UKF-based SF Implementation

The experimental evaluation of the proposed UKF-based SF is performed in two trials, the results of which are shown in Fig. 8 and Fig. . In these figures, the red cross and blue circle marks denote the position of Train A and Train B, respectively. It can be seen in these plots that the proposed UKF-based SF method effectively estimates the positions of both trains based on the encoder and RFID tags data. Furthermore, the proposed localization method accurately shows that the distribution of each mark is more dense in each of the defined station, indicating that each train is slowing down and/or comes to a complete stop.

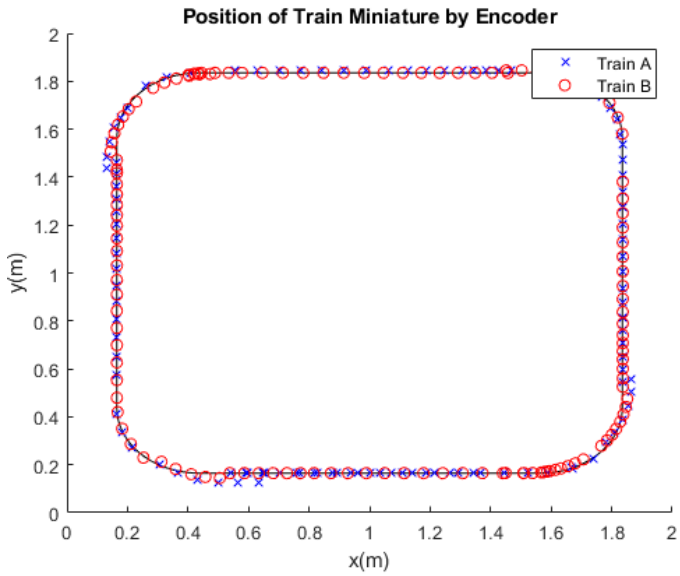

Fig. 8 UKF-based SF implementation result (trial 1).

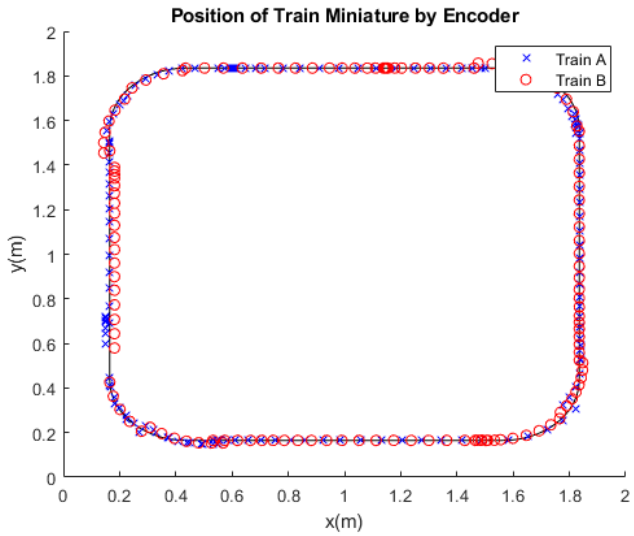

Fig. 9 UKF-based SF implementation result (trial 2).

We further compare the performance of the localization when using single sensor data (i.e. encoder) and that when using the SF method. Based on the resulting root mean square error (RMSE) as summarized in Table 2, the estimation errors of the SF-based localization method are significantly smaller than those based on single sensor data (both for individual train position estimation and in average). These results thus show that the the proposed UKF-based SF method has the potential to significantly improve the accuracy of the train localization system. The obtained high accuracy localization result is clearly very beneficial to support the CBTC implementation under the MBS scheme.

TABLE II
RMSE VALUE OF THE TRAIN LOCALIZATION TASK.

Root Mean Square Error Value (cm)					
Train	**Trial**	**x_enc**	**y_enc**	**x_ukf**	**y_ukf**
A	1	3.2	7.6	0.5	0.8
	2	5.6	4.3	0.8	0.8
B	1	3.3	3.4	0.7	0.7
	2	3.4	4.7	0.6	0.8
Average		**3.9**	**5.0**	**0.7**	**0.8**

B. Synchronization Control Implementation

The experimental evaluations of synchronization control are conducted to compare the train operation performance under the FBS scheme and that under MBS scheme with synchronization control. The results of these experiments are shown in Fig. and Fig. 11 which plot the position-time graphs of each train under the FBS and MBS schemes, respectively, for one full lap of the track. Both graphs in each of these figures essentially show the distance between the two trains in a signaling block.

It can be seen in these figures that the average inter-train distance in the FBS scheme is about 162 cm, whereas the inter-train distance in the MBS scheme that is equipped with the proposed synchronization control approach is only about 72 cm. These results thus show that, compared to the FBS scheme, the proposed MBS with synchronization control approach can reduce the operational headway up to 56%. These figures also show that the two trains in the MBS with

synchronization control scheme only need about seven (7) seconds to complete one full track, whereas the FBS one requires about 16 seconds to complete the same lap. These results thus clearly demonstrate the effectiveness of the proposed MBS with synchronization control approach in reducing both the train operational headway and travel time.

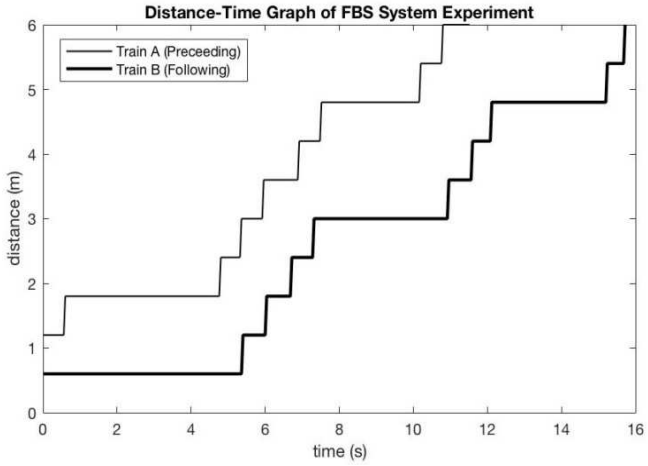

Fig. 10 Position vs. time graph of two trains under FBS scheme.

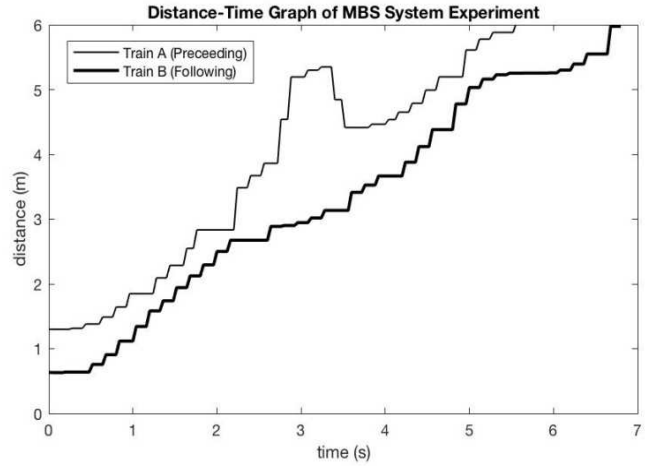

Fig. 11 Position vs. time graph of two trains under MBS scheme.

IV. Conclusion

This paper has reported the experimental results that were obtained when implementing a UKF-based SF approach for train localization and synchronization control of CBTC system under the MBS scheme. The presented localization results showed that the developed UKF-based SF method significantly improve the accuracy of the train position estimation. Furthermore, the experimental results of the MBS scheme implementation under the proposed synchronization control approach successfully reduce the train's operational headways and travel time. These results suggest that the SF-based synchronization control approach has a promising potential to improve the performance of CBTC systems.

Acknowledgment

This work was supported by the P3MI Program 2017 at Institut Teknologi Bandung, and by the Ministry of Research, Technology and Higher Education of the Republic of Indonesia under the Fundamental Research (PDUPT) scheme 2018.

References

[1] PT. Kereta Commuter Indonesia. (2019) Annual Report 2017. [Online]. Available: http://www.krl.co.id (retrieved on 10 April 2019).

[2] M.J. Lockyear,"Changing track: moving-block railway signaling," *IEE Review*, vol. 42, no. 1, pp. 21-25, 1996.

[3] C. Schifers and G. Hans, "IEEE standard for communications-based train control (CBTC) performance and functional requirements," in *Proc. Vehicular Technology Conf.*, pp. 1581-1585, 2000.

[4] W. C. Carreño, "Efficient driving of CBTC ATO operated trains," Ph.D. thesis, KTH Royal Institute of Technology, Stockholm Sweden, 2017.

[5] S. Thurn, W. Burgard, and D. Fox, *Probabilistic Robotics*, Boston, MA, USA: MIT Press, 2006.

[6] A. Mirabadi, N. Mort, and F. Schmid, "Application of sensor fusion to railway systems," in *Proc. IEEE MFI*, pp. 185-192, 1996.

[7] D. Veillard, F. Mailly, and P. Fraisse, "EKF-based state estimation for train localization," in *Proc. IEEE Sensors*, pp. 1-3, 2016.

[8] D. Lu and E. Schnieder, "Performance evaluation of GNSS for train localization," *IEEE Trans. Intell. Transp. Syst.*, vol. 16, no. 2, pp. 1054-1059, 2015.

[9] J. Marais, J. Beugin, and M. Berbineau, "A survey of GNSS-based research & developments for the European railway signaling," IEEE *Trans. Intell. Transp. Syst.*, vol. 18, no. 10, pp. 2602-2618, 2017.

[10] J. Otegui, A. Bahillo, I. Lopetegi, and L. E. Díez, "Evaluation of experimental GNSS and 10-DOF MEMS IMU measurements for train positioning," IEEE *Trans. Instrum. Meas.*, vol. 68, no. 1, pp. 269-279, 2019.

[11] K. Kim, S. Seol, and S. Kong, "High-speed train navigation system based on multi-sensor data fusion and map matching algorithm," *Int. J. Control Autom. Syst.*, vol. 13, no. 3, pp. 503-512, 2015.

[12] G. Muniandi and E. Deenadayalan, "Train distance and speed estimation using multi sensor data fusion," *IET Radar, Sonar, Nav.*, vol. 13, no. 4, pp. 664-671, 2019.

[13] F. Tschopp et al., "Experimental comparison of visual-aided odometry methods for rail vehicles," *IEEE Robot. Autom. Lett.*, vol. 4, no. 2, pp. 1815-1822, 2019.

[14] M. Lauer and D. Stein, "A train localization algorithm for train protection systems of the future," *IEEE Trans. Intell. Transp. Syst.*, vol. 16, no. 2, pp. 970-979, 2015.

[15] O. Heirich, "Bayesian train localization with particle filter, loosely coupled GNSS, IMU, and a track map," *J. Sensors*, Art. 2672640, 2016.

[16] J. Otegui, A. Bahillo, I. Lopetegi, and L. E. Díez, "A survey of train positioning solutions," *IEEE Sens. J.*, vol. 17, no. 20, pp. 6788-6797, 2017.

[17] E. A. Wan and R. V. D. Merwe, "The unscented Kalman filter for nonlinear estimation," in *Proc. IEEE ASSPCC*, pp. 153-158, 2000.

[18] S. J. Julier and J. K. Uhlmann, "A new extension of the Kalman filter to nonlinear system," in *Proc. SPIE SPSFTR Conf.*, pp. 182-194, 1997.

[19] S. J. Julier and J. K. Uhlmann, "Unscented filtering and nonlinear estimation,"*Proc. IEEE*, vol. 92, no. 3, pp. 401-422, 2004.

[20] S. J. Julier, "The scaled unscented transformation," in *Proc. American Control Conf.*, pp. 4555-4559, 2002.

[21] I. Faruqi et al., "Train localization using unscented Kalman filter–based sensor fusion," *Int. J. Sust. Transp. Technol.*, vol. 1, no. 2, pp. 35-41, 2018.

[22] Y. Y. Nazaruddin et al., "On using unscented Kalman filter based multi sensors fusion for train localization," in *Proc. ASCC*, 2019.

[23] R. Takagi, "Synchronization control of trains on the railway track controlled by the moving block signaling system," *IET Electric. Syst. Transp.*, vol. 2, no. 3, pp. 130-138, 2012.

[24] C. Bersani et al., "Rapid, robust, distributed evaluation and control of train scheduling on a single line track," *Control Eng. Pract.*, vol. 35, pp. 12-21, 2015.